

EXPERIMENTAL INVESTIGATION OF FRICTION AND WEAR BEHAVIOUR OF 304L STAINLESS STEEL SLIDING AGAINST DIFFERENT COUNTERFACE IN DRY CONTACT.

Olofinjana, B.^{1,2*}, Ajayi, O.², Lorenzo-Martin, C.², Ajayi. E. O. B.¹

¹ Department of Physics and Engineering Physics, Obafemi Awolowo University, Ile-Ife, 220005, Nigeria

² Tribology Section, Energy System Division, Argonne National Laboratory, 9700 S. Cass Avenue, Argonne, IL 60439, USA

* Corresponding Author, Tel: +234 8066762570, E-mail address: olofinb@oauife.edu.ng or olofinbolu@yahoo.co.uk

(Received: 26th Aug., 2016; Accepted: 13th Oct., 2016)

In this study, friction and wear behavior of 304L stainless steel sliding against different ball counterface under dry contact was investigated. Tests were conducted using a ball-on-flat contact configuration in reciprocating sliding with 440C stainless steel, Al alloy (2017) and bronze ball counterfaces under different loads. Detailed surface analysis was also done using 3-D profilometry technique and optical microscopy in order to determine wear mechanism and dimension. All the pairs exhibited initial rapid increase in coefficient of friction after which a variety of friction behavior, depending on the ball counterface, was observed. The flat and the ball counterface in 304L stainless steel-440C stainless steel pair showed wear that was proportional to applied load. In both 304L stainless steel-Al alloy (2017) and 304L stainless steel-bronze pairs, ball samples showed severe wear that was proportional to the applied load while material transfer from the different balls occurred in the flat. The study concluded that friction and wear were not material properties but a kind of responses that characterize a pair of surfaces in contact undergoing relative motion.

INTRODUCTION

Friction and wear have received a great deal of interest from researchers. This has led to the availability of vast quantity of information showing the complexity of tribology. To start with, friction can be defined as the motion resisting force between two surfaces in contact undergoing relative motion. The relative motion of two surfaces in contact induces non-conservative forces which give rise to loss of energy by resisting the motion. Wear, on the other hand, is a process of progressive detachment of material from one or both surfaces in relative motion. Mechanisms of material detachment involved in the process can be adhesion, abrasion, plastic deformation, fatigue, among others.

One area in which friction and wear has received extensive interest is that of industrial machinery and tools manufacturing. Equipment is expected to have longer life span under increasingly demanding harsh conditions. However, friction and wear have been a major impediment to this expectation. In addition, a lot of energy is lost trying to overcome this twin problem of friction and wear. With growing demand in cost savings, there is the need to understand the friction and wear response of different tribo-systems. Understanding this behavior will help in

determining the failure modes and life-span of the system components.

In any particular contact situation, there are always a number of different parameters that influence the friction and wear behavior of the tribo-system. For instance, it has been found that much of the characteristics of friction and wear are results of the properties of surfaces in contact (Farhet *et al.*, 1996; Kailas, 2003; Zhang *et al.*, 2006). Operating conditions such as temperature, normal load, contact geometry, sliding speed, relative humidity, vibration, working environment (Chowdhury and Helali, 2007; Chowdhury and Helali, 2008; Garbar, 1997; Davin, 2000; Bhushan and Kulkarni, 1996; Bregliozzi *et al.*, 2004; Emge *et al.*, 2009; Gaard *et al.*, 2010; Chen and Chang, 2003; Xia *et al.*, 2005; Lee *et al.*, 2011), and so on, can also influence friction and wear behavior of any tribo-system. Identifying and understanding the influence of these parameters will help in predicting and controlling both friction and wear.

Stainless steel is one of the major engineering materials with the widest diversity of applications. They are generally used in numerous applications that require corrosion resistance. The austenitic one

(e.g. 304L) have very good ductility and formability. They have been utilized extensively in food, chemical, medical and electrical industries and for machine parts (Bregliozzi *et al.*, 2004; Chen and Chang, 2003; Xia *et al.*, 2005). There are also attempts to extend their use in areas like microelectronic mechanical system (MEMS) (Lee *et al.*, 2011). Therefore a better understanding of the effect of material properties like hardness and surface roughness on friction and wear of stainless steel sliding against various materials is necessary. This will improve the ability to design working conditions and optimize material properties in order to minimize friction and wear. This study seek to investigate the friction and wear behavior of 304L stainless steel sliding against 440C stainless steel, Al (2017) alloy and bronze counterface in dry contact.

MATERIALS AND METHODS

Materials

As a result of its versatility in tribological applications where corrosion resistance is desirable, 304L stainless steel flat of dimension 25 x 50 x 6 mm was chosen for this study. The composition (in wt. %) of the 304L stainless steel used is 19.2 Cr, 11.3 Ni, 2.67 Mo, 1.86 Mn, 0.06 C and balance Fe. Its main properties are listed in Table 1. Surface preparation was carried out by manual wet grinding using silicon carbide papers from 60 to 120 grit giving 125 μ finish. The sample was then ultrasonically cleaned in acetone. The optical profilometry and micrograph of the 304L stainless steel after grinding is shown in Fig. 1 (a & b).

Table 1. Properties of 304L stainless steel

Property	Value
Density	8.00 g/cm ³
Melting point	1400-1450 °C
Elastic modulus	193 GPa
Tensile strength	500 MPa
Compression strength	210 MPa
Hardness	1.7 GPa (87R _B)
Poisson's ratio	0.3
Thermal conductivity	16.2 W/m K at 100 °C
Thermal expansion	17.2 x 10 ⁻⁶ /K at 100 °C
3-D surface parameter Ra	213 nm

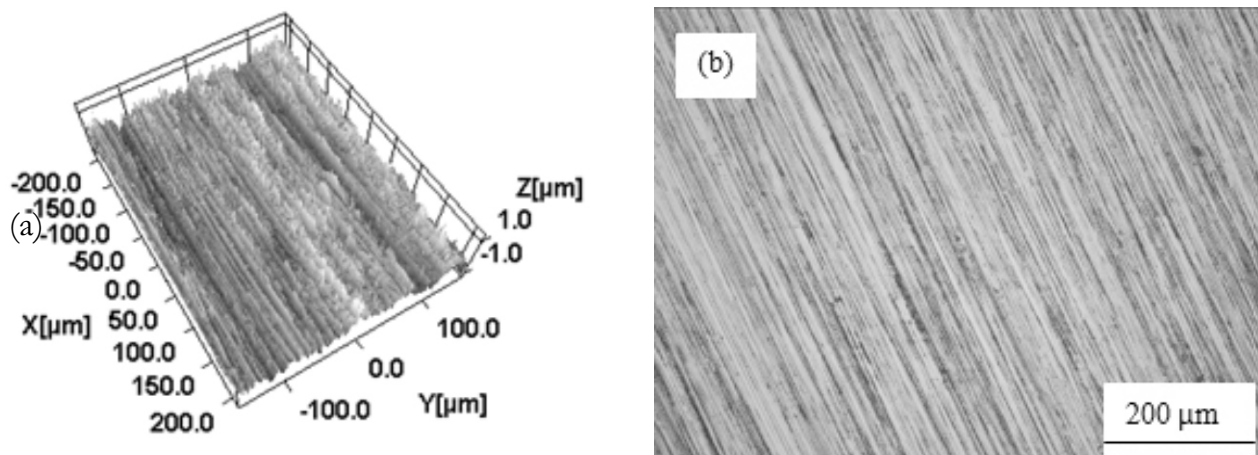


Fig. 1 (a) 3-D optical profile (b) optical micrograph of 304L stainless steel.

The ball counterface specimen are (i) commercially finished 440C steel with a composition of (in wt. %): 1.2 C, 18 Cr, 1 Mn, 0.75 Mo, 0.04 P, 1 Si, 0.03 S and balance Fe (ii) Al alloy (2017) with a composition of (in wt. %): 0.1 Cr, 3.5 Cu, 0.7 Fe, 0.4 Mg, 0.4 Mn, 0.2 Si, 0.15 Ti, 0.25 Zn, and balance Al (iii) bronze with

composition (in wt. %): 7 Pb, 6.7 Sn, 3 Zn and balance Cu. Some of the properties of the different ball counterface are listed in Table 2. 3-D optical profilometry of the balls are shown in Fig. 2. All the balls have a diameter of 12.7 mm (0.5 in).

Table 2. Some properties of the different ball counterface

Property	Stainless steel 440C	Al alloy (2017)	Bronze
Hardness	6.7 GPa (62R _C)	1.2 GPa (66R _B)	385 MPa (63R _C)
Elastic Modulus	200 GPa	72.4 GPa	97 GPa
Poisson's ratio	0.3	0.3	0.3
3-D surface parameter Ra	798 nm	736 nm	819 nm

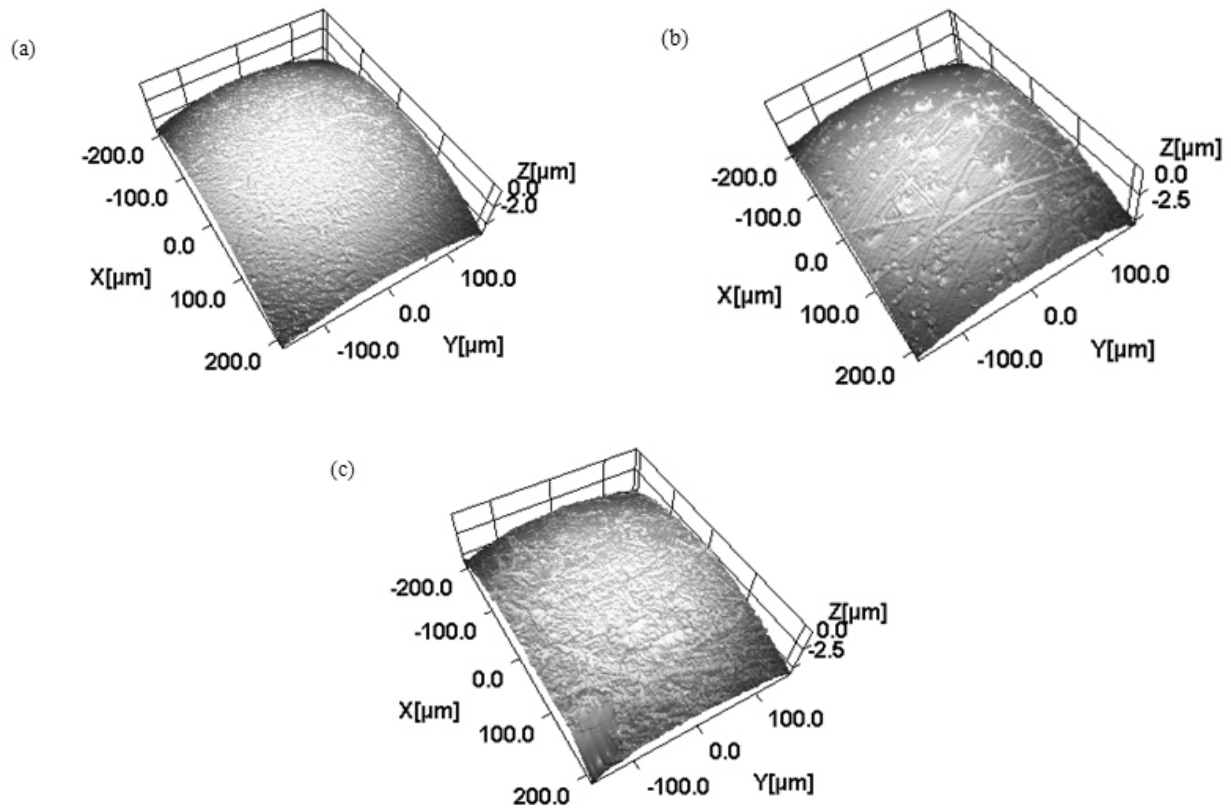


Fig. 2. 3-D optical profile of (a) 440C stainless steel (b) Al alloy (2017) (c) bronze ball counterface.

Friction and Wear Test

Friction and wear tests were conducted with a ball-on-flat contact configuration in reciprocating sliding using a high frequency reciprocating rig (HFRR). Fig. 3 shows the schematic diagram of the HFRR test rig. Tests were conducted with constant dead

weights of 5, 10 and 15 N at room temperature without intentional lubrication (dry). The reciprocating frequency was 1 Hz with a stroke length of 10 mm, equivalent to a linear speed of 1 cm/s. All tests were conducted for duration of 10 minutes.

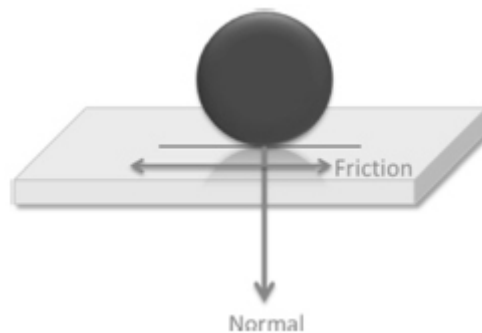


Fig. 3. Schematic diagram of ball-on-flat contact configuration under reciprocating sliding.

At the start of each test, flat and ball counterface samples were cleaned and mounted in their respective sample holders after which they were then mounted on the test rig. The frictional force was continuously monitored during each test from which the friction coefficient was calculated. At the conclusion of each test, the flat and ball counterface samples were thoroughly cleaned and wear dimensions was measured using 3-D profilometry technique. Worn surfaces were also characterized by optical microscopy to evaluate the wear and surface damage mechanism.

RESULT

Friction behavior

The friction variation with time during reciprocating sliding tests at normal loads of 5, 10 and 15 N for all the different pairs are shown in Fig. 4 (a-c). In the figure, the pairs of 304L stainless steel flat with 440C stainless steel ball, 304L stainless steel flat with Al alloy (2017) ball and 304L stainless steel flat with bronze ball are denoted by SS440C, Al2017 and Bronze respectively. At all the tested loads, the 304L stainless steel-bronze pair consistently showed the highest friction coefficient for all the tested pairs.

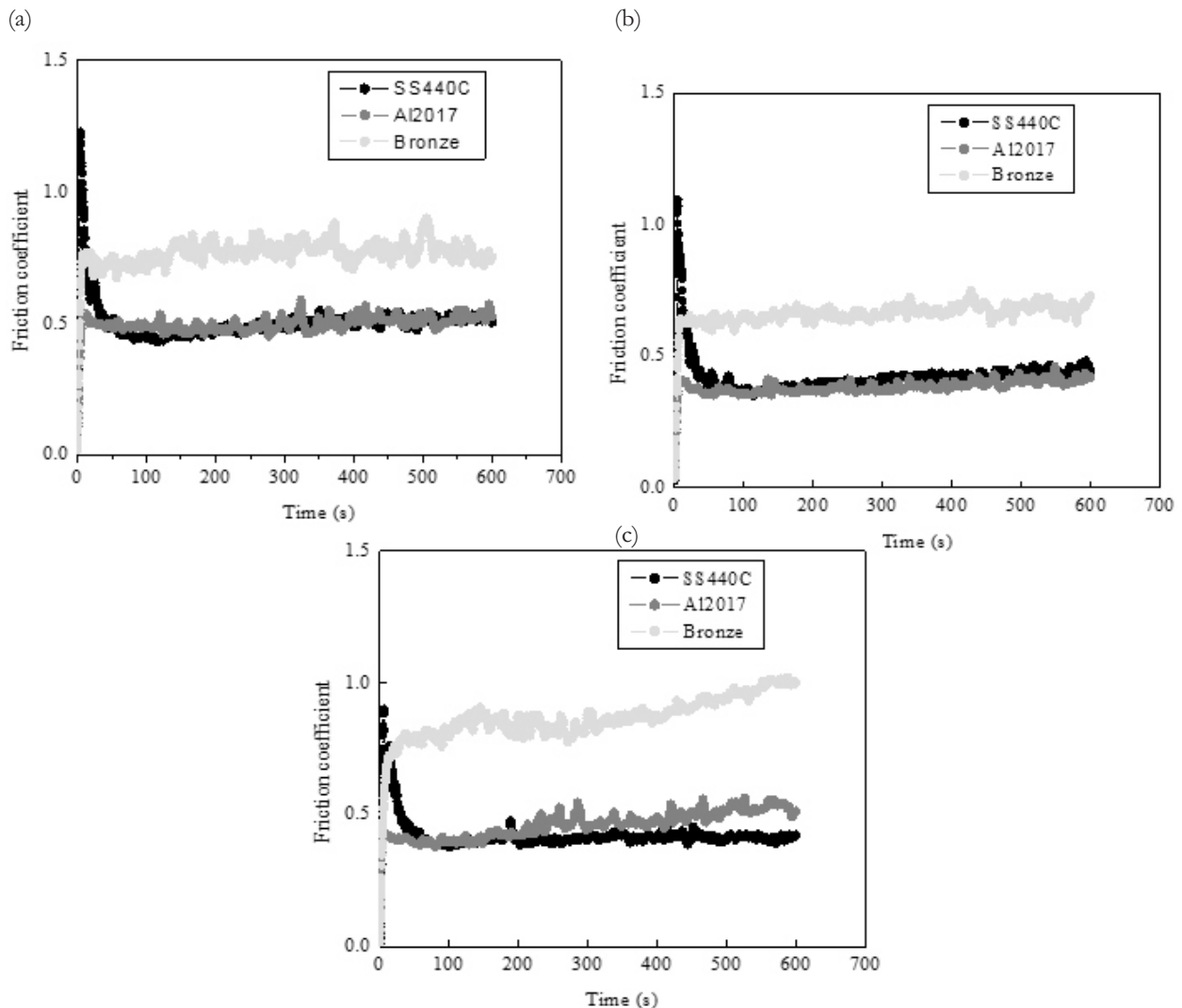


Fig. 4. Friction coefficient as a function of test duration at (a) 5 N (b) 10 N (c) 15 N for the pairs.

At 5 N load, for the 304L stainless steel-440C stainless steel pair, friction coefficient increased rapidly at the start of the test to a maximum value of about 1.25, followed by a gradual decrease to a value of 0.50 at about 50 s and remained nearly constant till the end of the test. In the case of the

304L stainless steel-Al alloy (2017) pair, friction coefficient increased rapidly at the start of the test to a nearly constant value of 0.50. The 304L stainless steel-bronze pair showed a rapid increase in friction coefficient to a value of 0.75 at the start of the test and thereafter remained unstable,

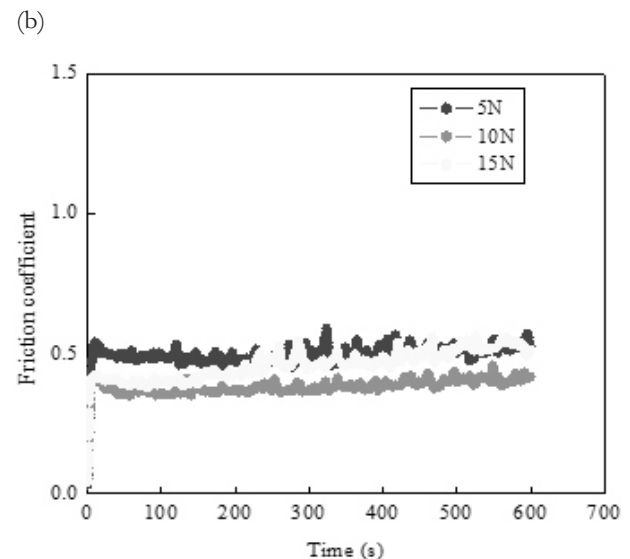
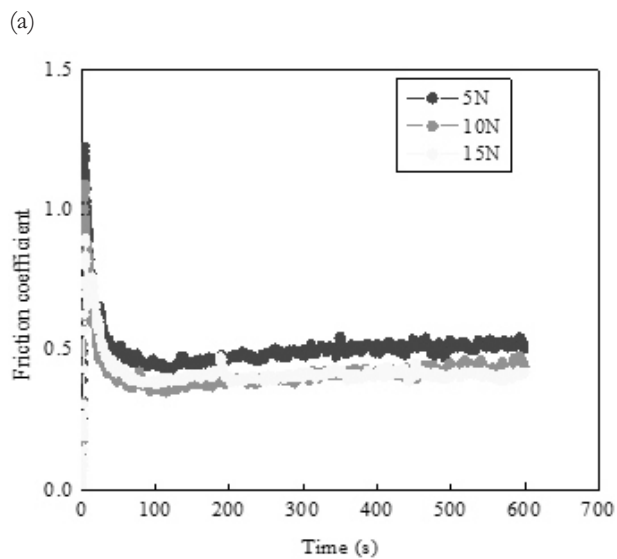
fluctuating between 0.75 and 0.90 for the remaining part of the test.

At 10 N, 304L stainless steel-440C stainless steel pair showed a rapid increase in friction coefficient at the start of the test to a maximum value of about 1.10. This was followed by a gradual decrease to a nearly constant value of 0.4. For 304L stainless steel-Al alloy (2017) pair, friction coefficient increased rapidly at the start of the test to a nearly constant value of 0.4. In the case of 304L stainless steel-bronze pair, the friction coefficient increased rapidly at the start of the test to a value of about 0.65. The friction coefficient then remained unstable, ranging between 0.60 and 0.65.

At 15 N load, 304L stainless steel-440C stainless steel pair showed a rapid increase in friction coefficient at the start of the test to a maximum value of 0.90, followed by a gradual decrease to a nearly constant value of 0.40. Frictional spike also occurred at about 200 s. For 304L stainless steel-Al alloy (2017) pair, friction coefficient increased rapidly at the start of the test to a value of about 0.40 which was nearly constant within the first 250

s and thereafter fluctuates between 0.50 and 0.55 for the rest of the test. In the case of 304L stainless steel-bronze pair, the friction coefficient increased to a value of 0.90 within the first 200 s of the test. This was then followed by a gradual increase to 1.00 at the end of the test.

Friction behavior under different loads for the three pairs is shown in Fig. 5. For the 304L stainless steel-440C stainless steel pair, trend of friction behavior is similar for all loads – rapid increase followed by gradual decrease to nearly constant value. Although the difference in steady state friction coefficient at all tested loads is not much, the 5 N load showed the highest friction coefficient while both 10 and 15 N load showed about the same steady state value in which case the 10 N load started with higher value than 15 N load during the run-in state. The trend of friction behavior in 304L stainless steel-Al alloy (2017) pair is also similar. 10 N load showed the lowest value while 15 N load showed a lower value than 5 N in the first 220 s. In the case of 304L stainless steel-bronze pair, 5 and 10 N load showed nearly the same trend, while the 15 N test showed a different pattern which has been described above.



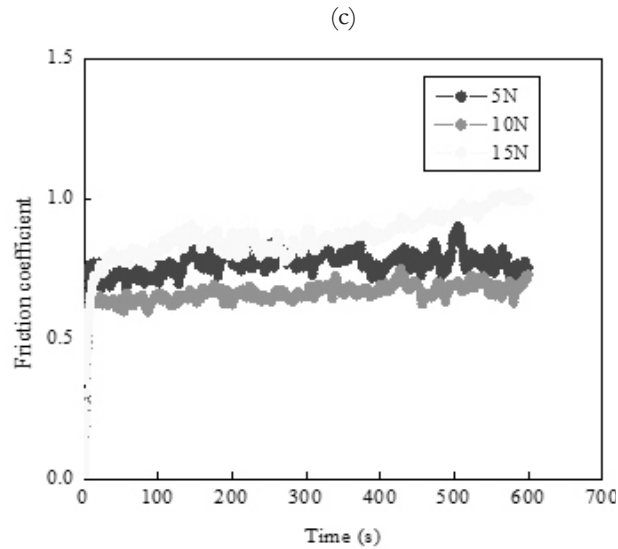


Fig. 5. Friction behavior under different loads for (a) 304L stainless steel-440C stainless steel (b) 304L stainless steel-Al alloy (2017) (c) 304L stainless steel-bronze pair.

Wear

For the pair of 304L stainless steel-440C stainless steel, all the 440C stainless steel balls showed the same features with different scales which increased as the load increases. Fig. 6 shows a typical 3-D optical profile (a) and the optical

micrograph (b) of the 440C stainless steel ball after the friction test. Some material removal in terms of wear with some roughening can be seen. Wear occurred by the formation and removal of oxide layer as indicated by dark patches in the track on the 440C stainless steel ball (Fig. 6b).

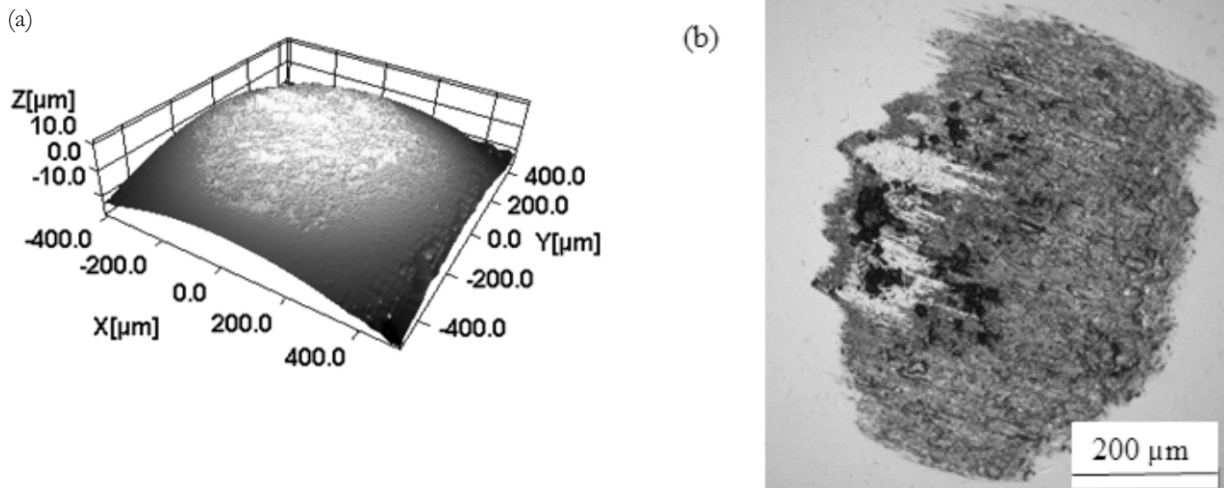


Fig. 6. (a) A typical 3-D optical profile (b) and the optical micrograph of the 440C stainless steel ball after the friction test.

Material removal i.e. wear proportional to applied load occurred in 304L stainless steel flat. Fig. 7 shows a typical 3-D optical profile (a) and optical micrograph (b) of the 304L stainless steel flat. A clear furrow was produced on the flat at all loads as illustrated by Fig. 7a. This surface damage occurs by abrasive wear as indicated by material pile up at

the edges of the track and deep scratches at the bottom of the furrow. Wear also occur by removal of oxide layer as shown by the dark patches in the optical micrograph. The optical micrograph also shows abrasive wear as indicated by scratches in the direction of sliding.

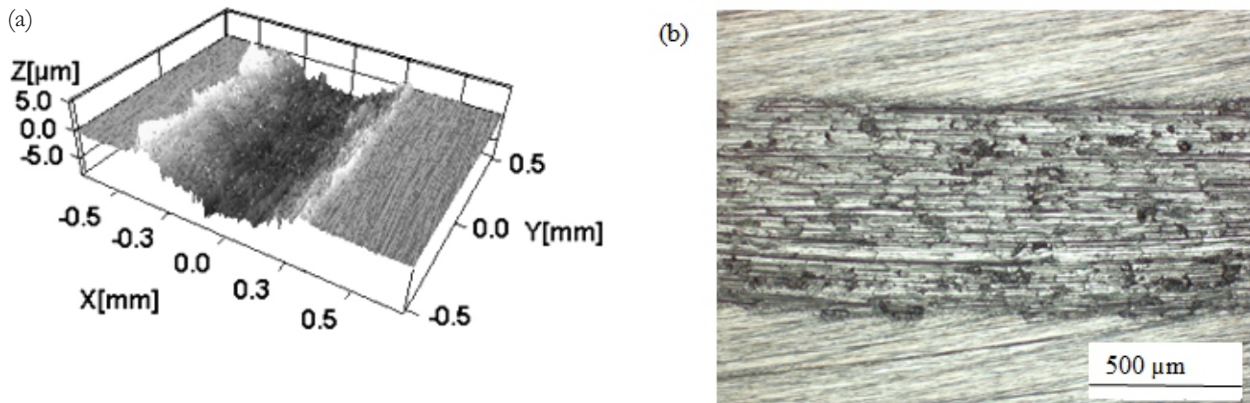


Fig. 7. (a) 3-D optical profile and (b) optical micrograph of flat sample for a typical AISI 304L stainless steel-440C stainless steel pair after test

Both 304L stainless steel-Al alloy (2017) and 304L stainless steel-bronze pairs showed the same features for both the flat and ball samples at all loads. All the ball samples showed severe wear that is proportional to the applied load. Fig. 8 shows 3-D optical profile (a) and optical micrograph (b) of such feature on a ball sample. As observed from the optical micrograph, wear occurred predominantly by abrasive mechanism as indicated by the deep scratches in the direction of sliding. Some dark patches can also be seen in the

wear tracks. This suggests that wear also occurred by formation and removal of oxide layers. However, the predominant mechanism was abrasion as the oxide formation and removal mechanism appeared to be very minimal. As for all the flats in these pairs, material transfer from the various balls occurred. Such transfer layer formed new tribolayers on the surface of the 304L stainless steel flat. Such tribolayers are shown in Figs. 9 and 10.

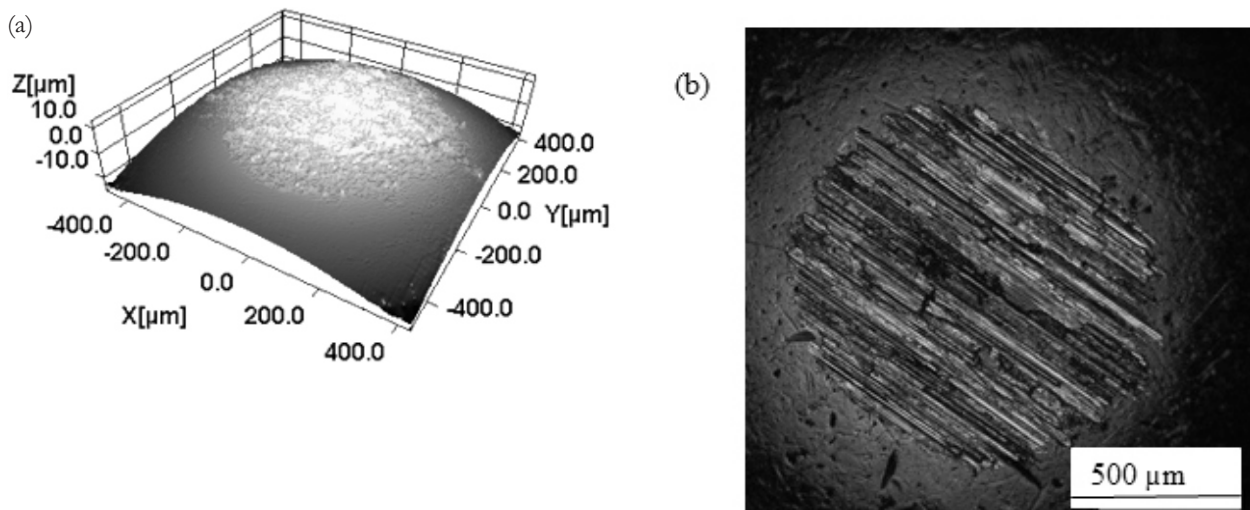


Fig. 8. (a) 3-D optical profile and (b) optical micrograph of bronze ball sample after friction test.

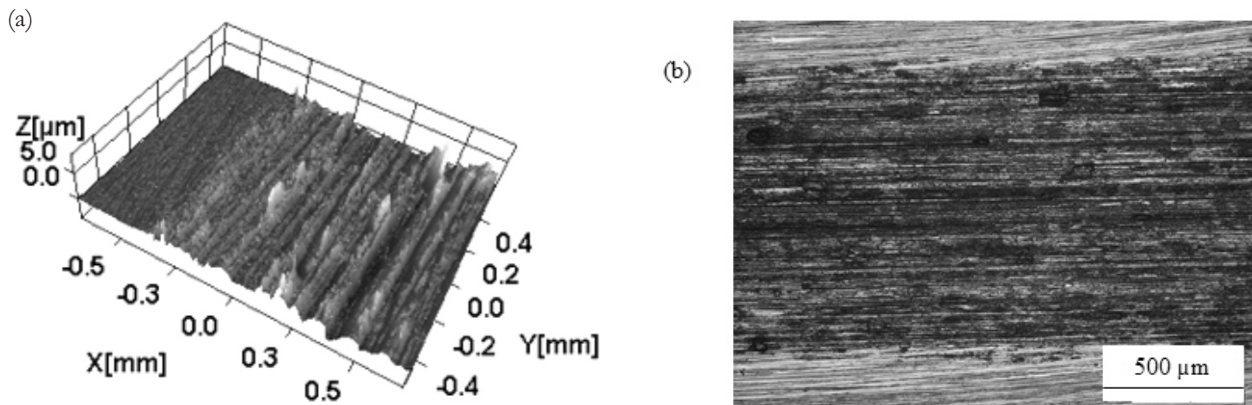


Fig. 9. (a) 3-D optical profile and (b) optical micrograph of flat sample for a typical 304L stainless steel-Al (2017) alloy pair after test

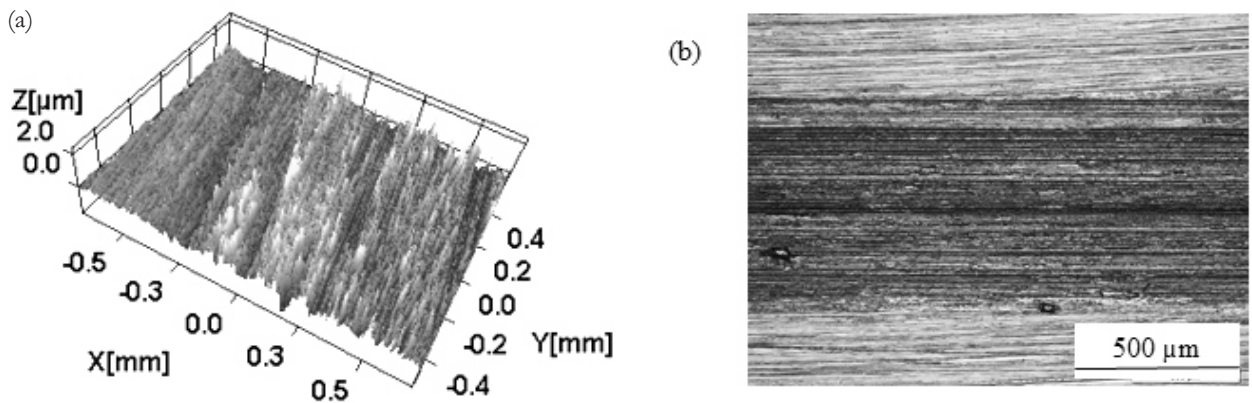


Fig. 10. (a) 3-D optical profile and (b) optical micrograph of flat sample for a typical 304L stainless steel-bronze pair after test

DISCUSSION

In all the sliding pairs tested at different loads, a range of frictional behavior was observed depending on the ball counter-face. The initial rapid increase in coefficient of friction exhibited by all the pairs at different loads is as a result of wear-in phenomena associated with the run-in period (Fazlalipour *et al.* 2012; Schon, 2004). This behavior may be as a result of ploughing effect which brings about roughening of the sliding pair, generating wear debris that can be entrapped (Bhushan, 2002). In addition, during run-in period, asperities are inter-locked together resulting in high resistance as sliding occurs thereby leading to rapid rise in coefficient of friction (Hutchings, 1992).

A number of different parameters can affect the friction and wear behavior of different sliding contact pair. Hardness defined as the resistance against plastic deformation, plays an important role. In the case of 304L stainless steel-440C

stainless steel pair, the 440C stainless steel ball counterface is harder than 304L stainless steel flat material (see Tables 1 and 2). Dry sliding of the hard 440C stainless steel ball counterface through a relatively soft 304L stainless steel flat leads to high shear stresses and strains at the contacting asperities. The resistance emanating from possible plastic deformation results in the ploughing effect (Holmberg *et al.*, 2007; Yamaguchi *et al.*, 2014) that causes the initial rapid increase as observed in the coefficient of friction. As the hard 440C ball counterface continue to move through the softer 304L flat surface, the high shear stresses formed exceeds the material strength of the 304L flat resulting in severe plasticity (Fig 7a), ploughing out grooves over depths that depends on the test conditions in the softer 304L flat (Rigney, 2000; Rainforth, 2000; Rainforth *et al.*, 2002; Alaneme *et al.*, 2015). The wear particles formed are abrasive and can be entrapped. As sliding continues, the wear debris can then create scratches in the softer 304L flat material while roughening or mild

abrasion in the hard 440C ball counterface can occur. The appearances of such scratches and furrows in the direction of sliding on the wear track of the 304L flat as can be seen in Fig. 7b, is an indication of abrasive wear. Once enough wear occurs, change in contact geometry from point non-conformal contact to a more conformal contact causes a gradual reduction in coefficient of friction (Olofinjana *et al.*, 2015) which then remains nearly constant till the end of the test. This type of friction behavior has also been observed for aluminum in contact with fiber composite (Schon, 2004). Sometimes, uneven plastic flow of asperities in the contact can produce frictional spikes as was observed in the 304L stainless steel-440C stainless steel pair tested at 15 N. Ajayi *et al.*, 2009, attributed such frictional spikes to frictional anisotropy in the grinding lay when the ball specimen slid parallel to the grinding ridges on the disc surface.

Furthermore, during dry sliding, new changes may occur at the interfaces of the two sliding bodies. Material transfer from one surface to another, wear debris generation and mechanical mixing of all these materials can be observed at the contacting surfaces. This leads to the formation of a tribolayer. Indeed it is well known that tribolayers consist of mixture of both material pair in contact, species from the environment, moisture, as well as oxides of metals (Schon, 2000). A tribolayer may have a beneficial or detrimental effect on both friction and wear depending on the thickness and adherence of the tribolayer (Stack and Mathew, 2004; Barrau *et al.*, 2003). The formation of this layer (as shown in Fig. 9) may be the reason for the nearly constant value of friction coefficient exhibited by the 304L stainless steel-Al (2017) pair after the run-in period. When the coefficient of friction began to stabilize, the contacting surfaces probably have a layer between them. The tribolayer can transmit load, separate contacting surfaces and velocity gradients. Some experimental conditions like contact pressure, sliding speed, can also affect the effectiveness of the tribolayer. Breakdown of the tribolayer at higher load of 15 N results in the fluctuations observed in the friction behavior after 250 s. As shown in Fig. 10, formation of tribolayer also occurred in 304L stainless steel-bronze pair, however, friction remained unstable

after the run-in period. This may be due to the poor adherence of the tribolayer on the 304L stainless steel flat. After run-in, wear debris from the softer ball accumulates to build up a transfer layer which is unstable and may eventually spall off to allow metal-metal interaction thereby leading to unstable friction behavior or rise in coefficient of friction.

CONCLUSION

Friction and wear behavior of 304L stainless steel sliding against different ball counterface under dry contact was investigated in this study. Friction and wear tests were conducted with a ball-on-flat contact configuration in reciprocating sliding using HFRR. Wear dimension and surface damage mechanisms were assessed using 3-D profilometry technique and optical microscopy.

All the pairs exhibited initial rapid increase in friction coefficient which was attributed to run-in processes. 304L stainless steel-440C stainless steel pair showed similar trend in friction behavior at all the tested loads. The nearly constant value after run-in period, observed in this pair was attributed to change in contact geometry from point non-conformal contact to a more conformal contact. 304L stainless steel-Al (2017) pair also exhibited similar trend in the friction behavior, however, the formation of tribolayer was observed. This tribolayer was responsible for the nearly constant value observed in the friction behavior after the run-in period. Tribolayer was also observed in the case of 304L stainless steel-bronze pair, but there was poor adherence of the tribolayer on the 304L flat and consequently led to unstable friction behavior after the run-in period.

The flat and the ball counterface in 304L stainless steel-440C stainless steel pair showed wear that was proportional to applied load. Wear occurred in the 304L stainless steel flat by a combination of severe plastic deformation and abrasion. On the other hand, wear occurred by the formation and removal of oxide layer together with some surface roughening in the 440C stainless steel ball. Both 304L stainless steel-Al alloy (2017) and 304L stainless steel-bronze pairs showed the same features for both the flat and the ball samples at all loads in terms of surface damage. Both the Al (2017) and bronze ball counterface samples

showed severe wear that was proportional to the applied load. Such wear occurred predominantly by abrasive mechanism with some cases of formation and removal of oxide layer. As for all the flats in these pairs, material transfer from the various balls occurred.

The results obtained showed that, the type of ball material can influence the friction and wear behavior of 304L stainless steel under dry contact condition. Consequently, friction and wear are not material properties but a kind of responses that characterize a pair of surfaces in contact undergoing relative motion.

ACKNOWLEDGMENTS

This work was supported by U.S. Department of Energy, Energy Efficiency and Renewable Energy, Office of Vehicle Technologies, under contract DE-AC02-06CH11357. One of the authors (BO) wishes to thank Obafemi Awolowo, Ile-Ife, Nigeria for granting him leave of absence to pursue this research.

REFERENCES

- Ajayi, O.O., Erck, R.A., Lorenzo-Martin, C. and Fenske, G.R. 2009. Friction Anisotropy under Boundary Lubrication: Effect of Surface Texture. *Wear*, 267(5-8), 1214-1219.
- Alaneme, K.K. and Sanusi, K.O. 2015. Microstructural Characteristics, Mechanical and Wear Behaviour of Aluminium Matrix Hybrid Composite Reinforced with Alumina, Rice Husk Ash and Graphite. *Engineering Science and Technology, an International Journal*, 18, 416.
- Barrau, O., Boher, C., Gras, R. and Rezai-Aria, F. 2003. Analysis of Friction and Wear Behaviour of Hot Tool Steel for Forging. *Wear*, 255(7-12), 1444-1454.
- Bhushan, B. 2002. Introduction to Tribology. *John Wiley & Sons Inc.* New York
- Bhushan, B. and Kulkarni, A.V. 1996. Effect of Normal Load on Microscale Friction Measurements. *Thin Solid Films*, 278(1), 49-56.
- Bregliozzi, G., Ahmed, S.I.U., Di Schino, A., Kenny, J.M. and Haefke, H. 2004. Friction and Wear Behaviour of Austenitic Stainless Steel: Influence of Atmospheric Humidity, Load Range, and Grain Size. *Tribology Letters*, 17(4), 697-704.
- Chen, F.S. and Chang, C.N. 2003. Effect of CH₄ Addition on Plasma Nitrocarburizing of Austenitic Stainless Steel. *Surface and Coating Technology*, 173(1), 9-18.
- Chowdhury, M.A. and Helali, M.M. 2007. The effect of Frequency of Vibration and Humidity on the Wear Rate. *Wear*, 262(1-2), 198-203.
- Chowdhury, M.A. and Helali, M.M. 2008. The Effect of Amplitude of Vibration on the Coefficient of Friction for Different Materials. *Tribology International*, 41(4), 307-314.
- Davim, J.P. 2000. An Experimental Study of the Tribological Behaviour of Brass/Steel Pair. *Journal of Materials Processing Technology*, 100(1-3), 273-277.
- Emge, A., Karthikeyan, S. and Rigney, D.A. 2009. The Effects of Sliding Velocity and Sliding Time on Nanocrystalline Tribolayer Development in Copper. *Wear*, 267(1), 562-567.
- Farhet, Z.N., Ding, Y., Northwood, D.O. and Alpas, A.T. 1996. Effect of Grain Size on Friction and Wear of Nanocrystalline Aluminium. *Material Science and Engineering A-Structure*, 206(2), 302-313.
- Fazlalipour, F., Shakib, N., Shokuhfar, A. and Nushari, M.N. 2012. Effect of Nitrocarburizing Treatment on Wear Mechanism and Friction of Steel/WC-Co Sliding Couple. *Journal of Tribology*, 134(4), 1-6.
- Gaard, A., Hallback, N., Krakhmalev, P. and Bergstrom, J. 2010. Temperature Effect of Adhesive Wear in Dry Sliding Contact. *Wear*, 268(7-8), 968-975.
- Garbar, I.I. 1997. The Effect of Load on the Structure and Wear of Friction Pair Materials: Example of Low Carbon Steel and Copper. *Wear*, 205(1-2), 240-245.

- Holmberg, K., Ronkainen, H., Laukkanen, A. and Wallin, K. 2007. Friction and Wear of Coated Surfaces - Scale, Modelling and Simulation of Tribomechanisms. *Surface and Coating Technology*, 202(4-7), 1034-1049.
- Hutchings, I.M. 1992. Tribology: Friction and Wear of Engineering Materials. *Edward Arnolds*. London
- Kailas, S.V. 2003. A Study of the Strain Rate Microstructural Response and Wear of Metals. *Journal of Materials Engineering and Performance*, 13(6), 629-637.
- Lee, C.Y., Lin, C.H. and Lo, Y.M. 2011. Fabrication of a Flexible Micro Temperature for Micro Reformer Applications. *Sensors*, 11(4), 3706-3716.
- Olofinjana, B., Lorenzo-Martin, C., Ajayi, O.O. and Ajayi, E.O.B. 2015. Effect of Laser Surface Texturing (LST) on Tribochemical Films Dynamics and Friction and Wear Performance. *Wear*, 332-333 1225-1230.
- Rainforth, W.M. 2000. Microstructural Evolution at the Worn Surface: A Comparison of Metals and Ceramics. *Wear*, 245(1-2), 162-177.
- Rainforth, W.M., Leonard, A.J., Perrin, C., Bedolla-Jacuinde, A., Wang, Y., Jones, H. and Luo, Q. 2002. High Resolution Observations of Friction-Induced Oxide and its Interaction with the Worn Surface. *Tribology International*, 35(11), 731-748.
- Rigney, D.A. 2000. Transfer, Mixing and Associated Chemical and Mechanical Processes During the Sliding of Ductile Materials. *Wear*, 245(1-2), 1-9.
- Schön, J. 2000. Coefficient of Friction of Composite Delamination Surfaces. *Wear*, 237(1), 77-89.
- Schön, J. 2004. Coefficient of Friction for Aluminium in Contact with a Carbon Fibre Epoxy Composite, *Tribology*, 37(5), 395-404.
- Stack, M.M. and Mathew, M.T. 2004. Mapping the Micro-Abrasion Resistance of WC/Co Based Coating in Aqueous Conditions. *Surface and Coating Technology*, 183(2-3), 337-346.
- Xia, Y., Hu, J., Zhou, F., Lin, Y. Qiao, Y. and Xu, T. 2005. Friction and Wear Behaviour of Plasma Nitride 1Cr18Ni9Ti Austenitic Stainless Steel under Lubrication Condition. *Material Science and Engineering A*, 402(1-2), 135-141.
- Yamaguchi, K., Sasaki, C., Tsuboi, R., Atherton, M., Storlacki, T. and Sosaki, S. 2014. Effect of Surface Roughness on Friction Behaviour of Steel under Boundary Lubrication, *Journal of Engineering Tribology*, 10, 1-5.
- Zhang, Y.S., Han, Z., Wang, K. and Lu, K. 2006. Friction and Wear Behaviours of Nanocrystalline Surface Layer of Pure Copper. *Wear*, 260(9-10), 942-948.